LA-UR-13-24002

Title: COUPLED EULER-LAGRANGE SIMULATION OF THE JOLT HE EVENT AND RELEVANCE TO THE SHOCK PHYSICS EXPERIMENTS

Author(s): Steedman, David W.

Intended for: Report

Issued: 2013-05-31

COUPLED EULER-LAGRANGE SIMULATION OF THE JOLT HE EVENT AND RELEVANCE TO THE SHOCK PHYSICS EXPERIMENTS

David W. Steedman

Los Alamos National Laboratory, Earth and Environmental Sciences Division

ACKNOWLEDGEMENT

The Source Physics Experiments (SPE) would not have been possible without the support of many people from several organizations. The author (s) wish to express their gratitude to the SPE working group, a multi-institutional and interdisciplinary group of scientists and engineers from National Security Technologies (NSTec), Lawrence Livermore National Laboratory (LLNL), Los Alamos National Laboratory (LANL), Sandia National Laboratories (SNL), the Defense Threat Reduction Agency (DTRA), and the Air Force Technical Applications Center (AFTAC). Deepest appreciation to Mssrs. Bob White and Ryan Emmitt (NSTec) for their tireless support on the seismic array and to the University of Nevada, Reno (UNR) for their support with the seismic network and data aggregation. Thanks to U.S. Geological Survey (USGS), the Incorporated Research Institutions for Seismology (IRIS) Program for Array Seismic Studies of the Continental Lithosphere (PASSCAL) Instrument Center, Lawrence Berkeley National Laboratory (LBNL), and Dr. Roger Waxler (University of Mississippi) for instrumentation partnership. The author(s) also wish to thank the National Nuclear Security Administration (NNSA), Defense Nuclear Nonproliferation Research and Development (DNN R&D) for their sponsorship of the National Center for Nuclear Security (NCNS) and its Source Physics Experiment (SPE) working group. This work was sponsored by the NNSA under award number DE-AC52-06NA25946.

INTRODUCTION

The NNSA is conducting a series of high explosive (HE) tests – the Source Physics Experiments – at the National Nuclear Security Site (NNSS). These experiments are intended to investigate the generation of geophysical signals from controlled sources. These signals will aid in the development of physics-based models to aid in the discrimination of signals emitted from these and other possible sources, such as earthquakes and clandestine nuclear events.

One aspect of study is the effect of local geology on propagated signals and, in particular, whether local joint sets alter the shock front. We study this phenomenological aspect by performing a numerical simulation of the JOinted Limestone Tests (JOLT) conducted during the Defense Threat Reduction Agency (DTRA) Hard and Deeply Buried Target (HDBT) Advanced Concept Technology Demonstration (ACTD) program.

THE TTD ACTD

The DTRA conducted the TTD ACTD program in an effort to identify candidate computational schemes for replacing the semi-theoretical method in use at the time for estimating vulnerability of tunnels to nuclear attack. The program combined a series of experiments with numerical analysis, and included an extensive verification and validation effort of the various codes under study. The test series included laboratory-scale experiments.

These laboratory-scale experiments, referred to as the JOinted Limestone Tests (JOLT), were conducted in 2006 (Ref. 1). Constructed and carried out at SRI International, these tests included an explosive source to create shock through a jointed, layered limestone test bed which included two tunnels. Computation methods generally included performing an Eulerian calculation of the source region to develop loading conditions for driving the rock response. Depending on the modeling group the rock region was modeled using Arbitrary Lagrangian-Eulerian (ALE), Lagrangian, or discrete elements. The joints/layers were variously modeled as contact surfaces, contact elements, and continuum elements with contact properties. The simulations had limited success in replicating both active data and tunnel damage in the tests.

Recent developments in the Abaqus® code allow simulation of these events using a fully coupled Euler-Lagrange approach. Simultaneous solution of the Eulerian source region and the Lagrangian rock allows more accurate modeling. A robust contact algorithm allows for modeling of the individual limestone blocks as separate continuum entities. In this paper we present results of a JOLT simulation using this approach and compare these results to the test data.

JOLT

The JOLT test bed, illustrated in Figure 1, includes 24-in (0.6096-m) square, ½-in (0.0127 m) thick Salem limestone plates, cracked at 0.0127-m intervals in orthogonal directions to form cubes. Sixty-five cracked plates were stacked to form imbricate joints in layers. Large blocks of limestone were placed above and below the plates, and grout and concrete regions were poured around the test bed to extend the boundaries. A 0.680-kg sphere of Composition B (CompB) explosive was detonated above the layered test bed. Two 4-in (0.1016-m) diameter cylindrical holes were drilled through the plates to simulate tunnel facilities. Data acquisition included accelerometers and stress gauges to provide active data, and post-test deconstruction to document damage and deformation of the test bed.

SIMULATION

The JOLT test bed was modeled using the fully coupled Euler-Lagrange capability of Abaqus® (Abaqus/CEL). This approach uses two solution domains, an Euler domain and a Lagrange domain, solved simultaneously with solution transfer between domains to allow full two-way, element-by-element, time step-by-time step coupling in a multi-physics approach. An Euler domain was used for the high-deformation explosive source region while the Lagrange domain was used throughout the rock test bed to accommodate the complex constitutive response as well as the block-to-block contact. Figure 2 illustrates the ¼-symmetry Abaqus/CEL model.

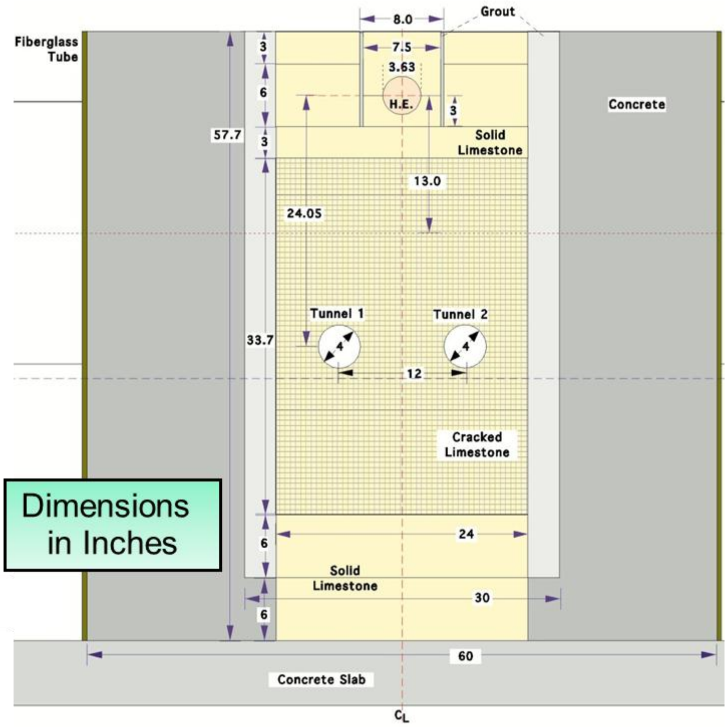

Figure 1: JOLT test bed.

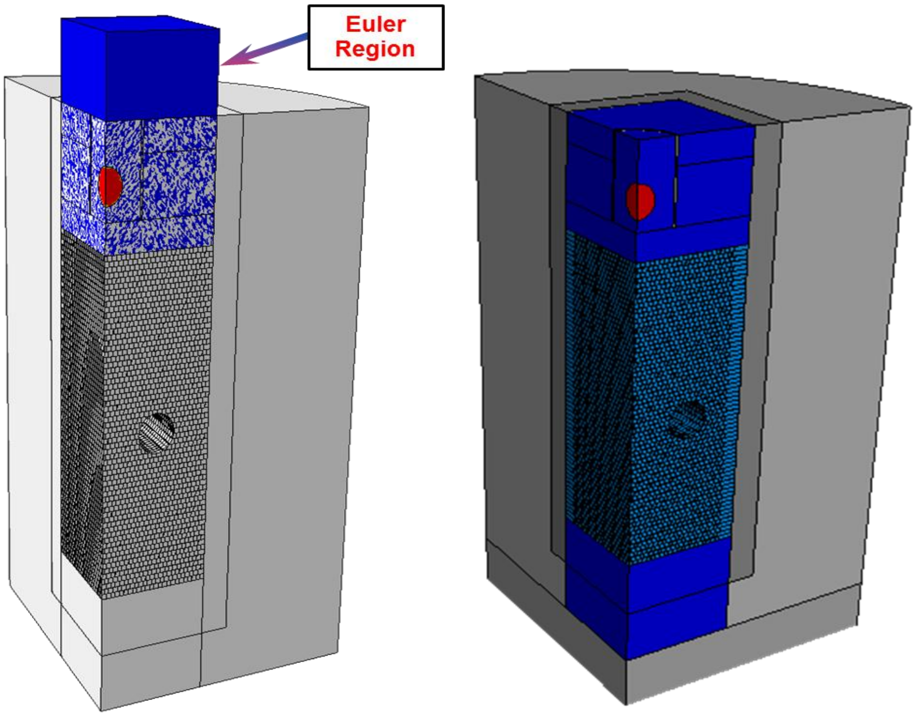

Figure 2: CEL model.

The Euler domain included the explosive, with a void region that overlaps the surrounding rock. Contact occurs between the Eulerian material surface (in this case the detonation products) and the Lagrange solid. The explosive was modeled as a JWL equation-of-state (EOS) with published constants for CompB (Ref. 2). The EOS was center-detonated with a programmed burn.

The Lagrange domain included the limestone blocks, the cracked limestone plates, the grout and the concrete. In ¼-symmetry, this makes 576, cubes per layer, or 37,440 cubes in 65 layers, minus those cubes removed to accommodate the tunnels. Each limestone cube included a 3 x 3 x 3 mesh of continuum elements.

The limestone was modeled using the Abaqus® brittle cracking failure model. This model assumes a linear elastic response prior to cracking. Brittle cracks are initiated as Mode I fractures (*i.e.*, tensile softening). After crack initiation both Mode I and Mode II (*i.e.*, shear softening) occur. Total failure is defined after sufficient cracking strain (crack opening) is achieved. Properties for this model (*i.e.*, elastic modulus: E=30 GPa, Poisson's ratio: ν=0.3, bulk density, ρ=2710 kg/m3, tensile strength, q_t=8 MPa, and cracking strain at failure, ε^f_{cr}=0.001) were based on data for Salem limestone (Ref. 3). There are some limitations of this model, such as the lack of an elastic-plastic pressure/excess compression EOS to model crush behavior. Nonetheless, simulation of a prior test of this nature (Ref. 4) demonstrated that a brittle model provided better replication of rock damage than did elastic-plastic, ductile yield models developed for this material at higher confining pressures (Ref. 5).

The block contacts were modeled using simple Coulomb friction with non-compliant ("hard") normal contact. The plate surfaces were ground smooth, while the vertical surfaces were rough because they were formed by cracking. A friction coefficient of 1 in a general contact domain was used as a first order compromise between the two extremes. A more accurate differentiation between the two types of surfaces might result in an improved model.

RESULTS

The JOLT simulation was run for a 15-ms duration. This is sufficient to capture the dynamic response of the test bed, although complete kinematic response to static equilibrium would take considerably more time.

A comparison between the post-test photograph of the top of the cratered test bed and the final configuration of the top of the model is included in Figure 3. Mirror imaging was performed on the symmetry boundaries in the post-processor to create a 360^o image. The following similarities between the two images are observed:

1. The crater extends to the grout/concrete interface.
2. There are regions of closely spaced radial cracks intermittent with regions of longer undamaged pieces of concrete. In the simulation, radial cracks emanate from the square corners of the grout/concrete interface due to stress concentrations at corners.

3. The side of the experiment furthest from the camera appears to have experienced a more complete blow-out indicating that there was not perfect symmetry in the experiment.

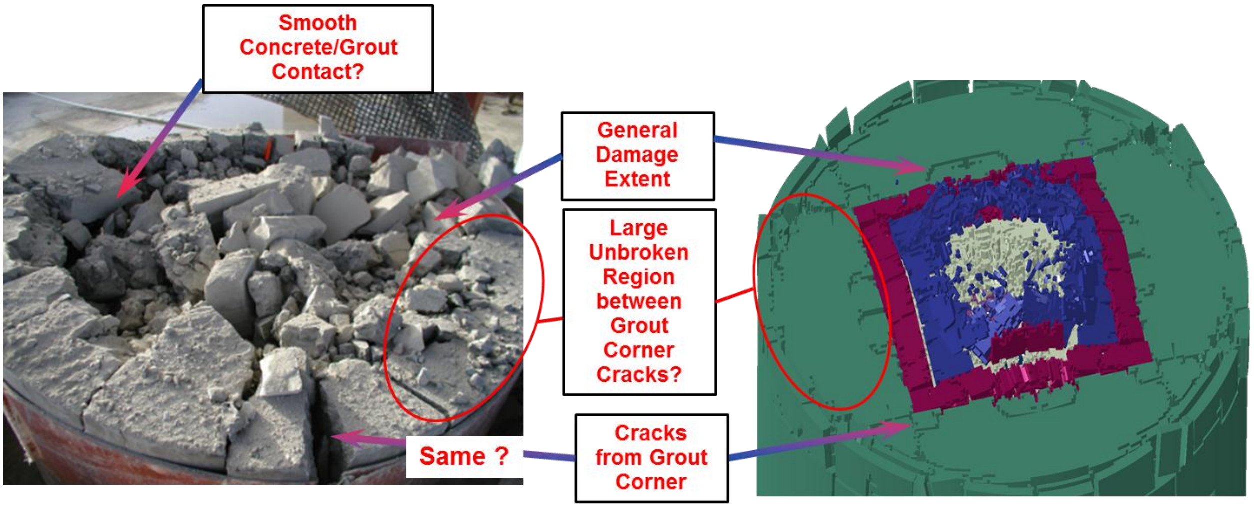

Figure 3: Final configuration of top of test bed; left: test bed, right: simulation.

A comparison between a post-test photograph of the top of layer 60 and the final computed configuration of the top of layer 60 in the model is included in Figure 4. The following observations can be made:

1. Both show a circular “dimpled” region in the center of the plate.
2. Both show a larger circular region of cracking. There is a difference, though, in that the test caused radial cracking while the computed cracks have no distinct pattern. Note that the “cross” pattern in the simulation exists on the symmetry boundaries of the simulation suggesting a concentration of shock reflections in perfect symmetry which, as we observed earlier, did not appear to exist in the test.

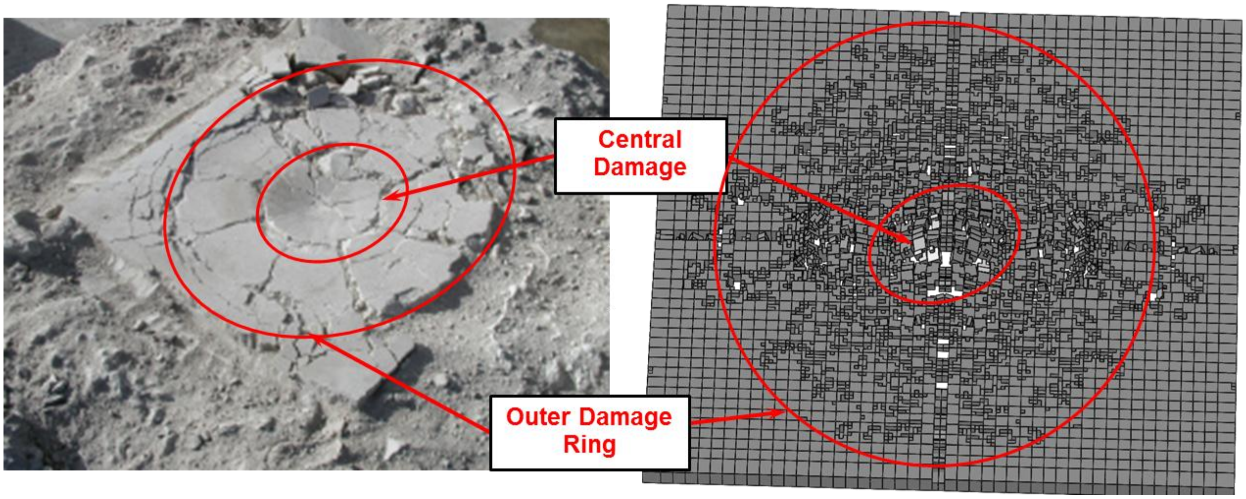

Figure 4: Plate 60 damage; left: test, right: simulation.

Figure 5 is a plot of peak vertical stress vs. depth down-axis from the explosive center, including both data and computed values. The simulation is close to the data near to the source but there is increasing divergence with depth. This less steep attenuation in the simulation is likely due to the lack of shock absorbing compression in the rock EOS.

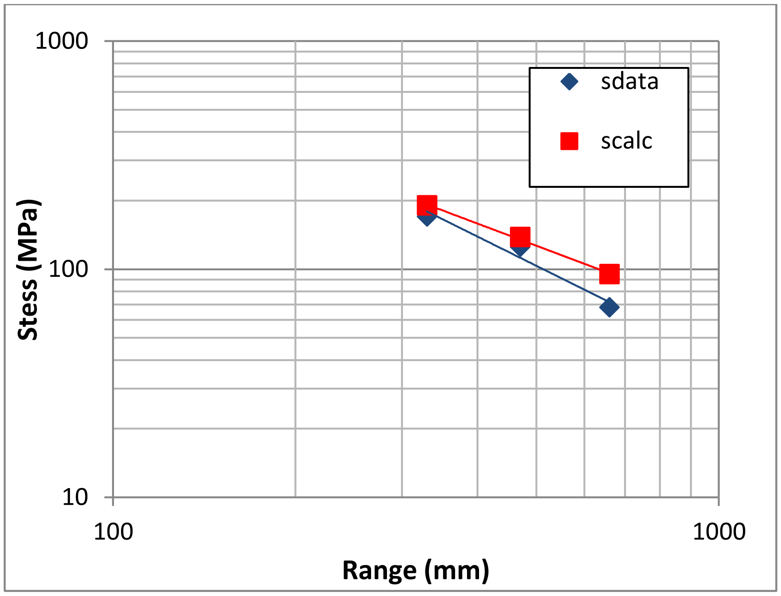

Figure 5: Recorded and calculated peak vertical stress with depth.

A comparison of test bed and computed tunnel damage is shown in Figure 6. The photographs show the rubble in the tunnel (left) and the arching caused by loss of support through creation of the rubble (center). The balloon in the center photograph was inserted into the tunnel after the event to preserve the final configuration. Figure 6 also includes the final configuration of the tunnel in the simulation, and shows contours of scalar velocity. Figure 7 provides a cross-section damage map down the tunnel axis and a similar view of the simulated tunnel final configuration without any contoured variable. In summary:

1. In the test, the first row or two above the tunnel crown and near to the center of the test bed collapsed. Layers above this remained in place due to arching.
2. In the simulation, the first two layers above the crown have collapsed by the end of the simulation. We assume that cubes with no, or nearly no, velocity (blue contours) at this point in the calculation would not undergo addition displacement with additional simulation time. It follows that no additional layers will collapse into the tunnel. However, the collapsed cubes in the simulation extend further down the axis than in the test. It is likely that proper modeling of the cracked vertical contacts could isolate this damage to the central tunnel region.
3. Generally, these comparisons suggest an accurate simulation.

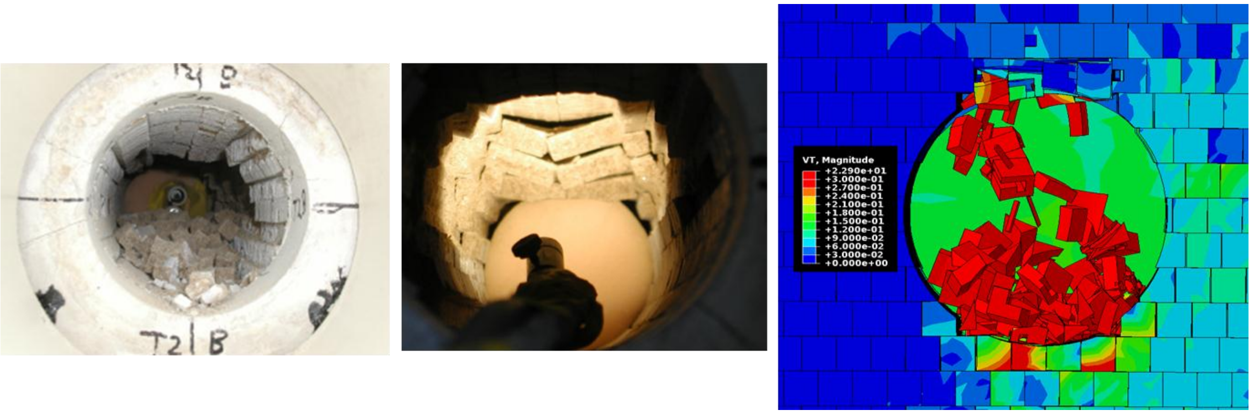

Figure 6: Damage down tunel axis; left: test, right: simulation.

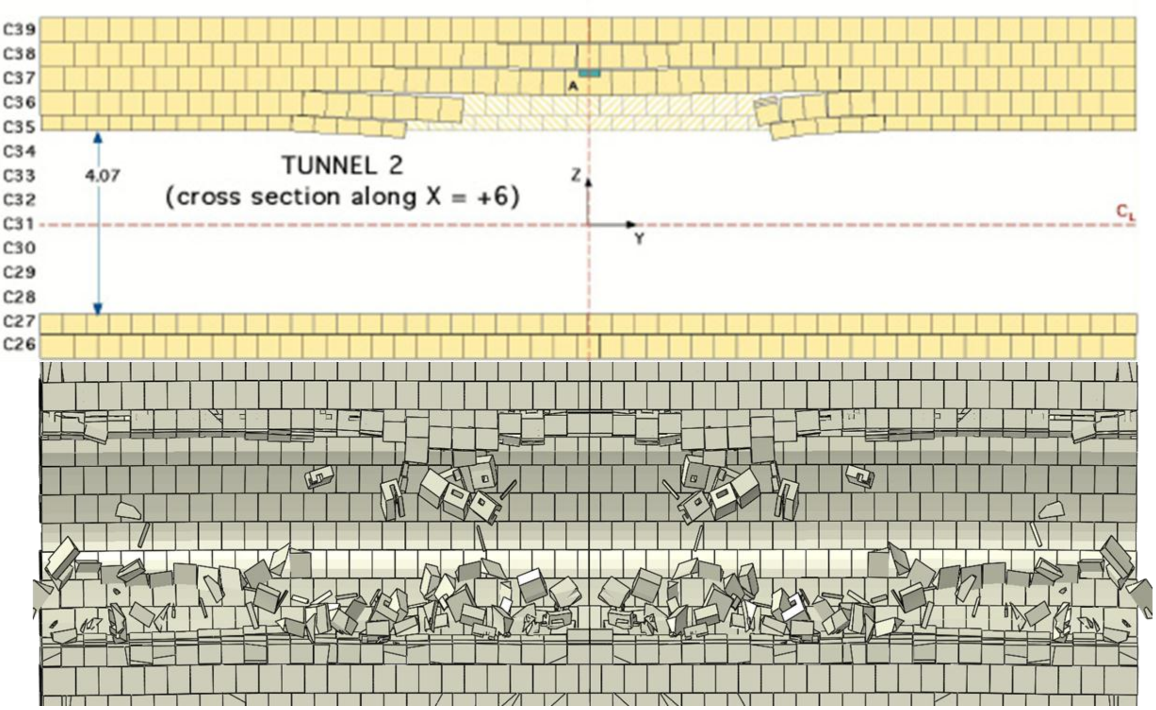

Figure 7: Damage down axis; top: test, bottom: simulation.

Finally, Figure 8 provides snapshots of scalar velocity contours at two intermediate times in the simulation. The left figure is at 100 μs simulation time. This figure demonstrates that the spherical shock front generated by a spherical charge remains spherical despite the frequent occurrence of three joint sets. The right figure illustrates the shock front at 200 μs simulation time after it has passed the tunnels.

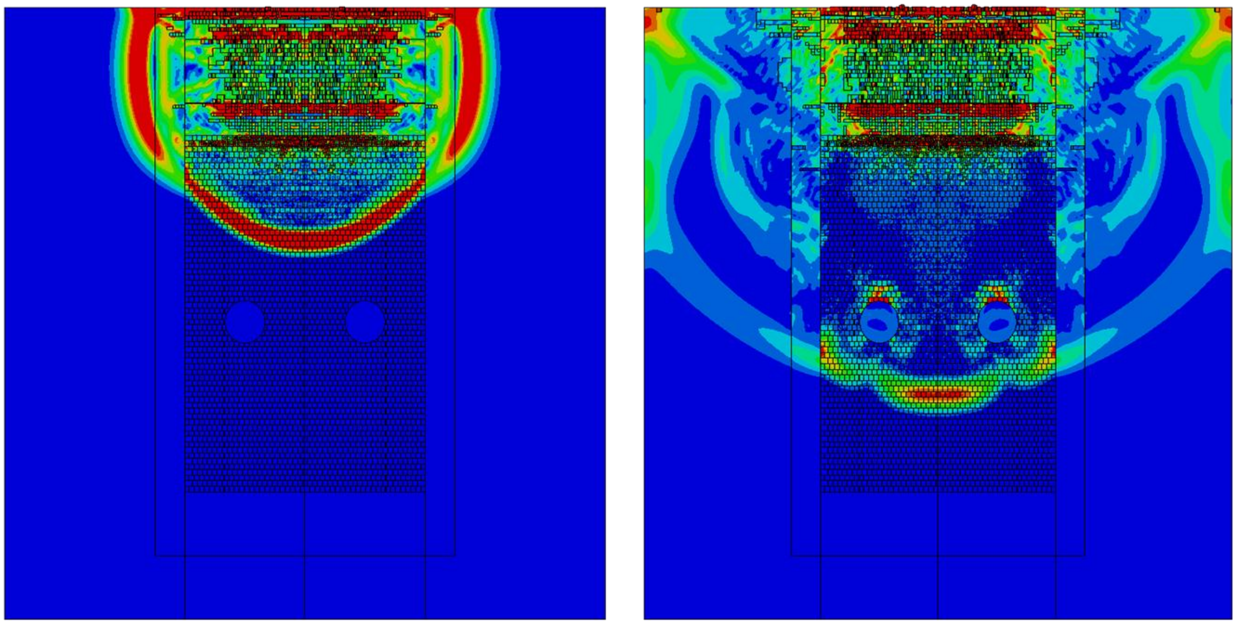

Figure 8: Computed scalar velocity contours; left: 100 μs, right 200 μs.

SPE GROUND SHOCK

These JOLT results are of interest when considering phenomenology in the SPE tests bed. As noted previously, this test bed has several local joint sets and there is interest in whether these joint sets alter the phenomenology of ground shock from an explosive source. The SPE events are a very well instrumented series. However, as an *in situ*, full-scale test bed there is less opportunity to compare response between simulation and experiment as we accomplished with JOLT.

However, the near field accelerometer data for SPE-2 can be analyzed to review shock front shape. To achieve an accurate representation of this parameter we used the accelerometer data that were corrected for canister rotation (Ref. 8). A review of the SPE test bed design (Figure 9) reveals that the set of near field instruments were arrayed at three different elevations and at two different ranges. But the general shape of the shock front can be accurately portrayed by projecting all instruments to the shot plane. For example, the radial peak for the gauge at a horizontal distance of 10 m and 30.48 m (100 ft) above the shot has a slant range of 32.08 m. For a spherical shot the outward motion on the horizontal shot plane at that radius (32.08 m) will have an equal value. It follows that a spherical shock front will contour as circles on that horizontal plane.

This process was accomplished, and the results are plotted in Figure 10. The contours conform to the expectations of a circular pattern. The pattern would ideally be centered on the shot ground zero (“GZ”). That is, the highest velocity would obviously be at the source. But the limited number of data points causes a shift in the pattern so that it centers on the highest velocity value nearest to the shot, at canister 3-2.

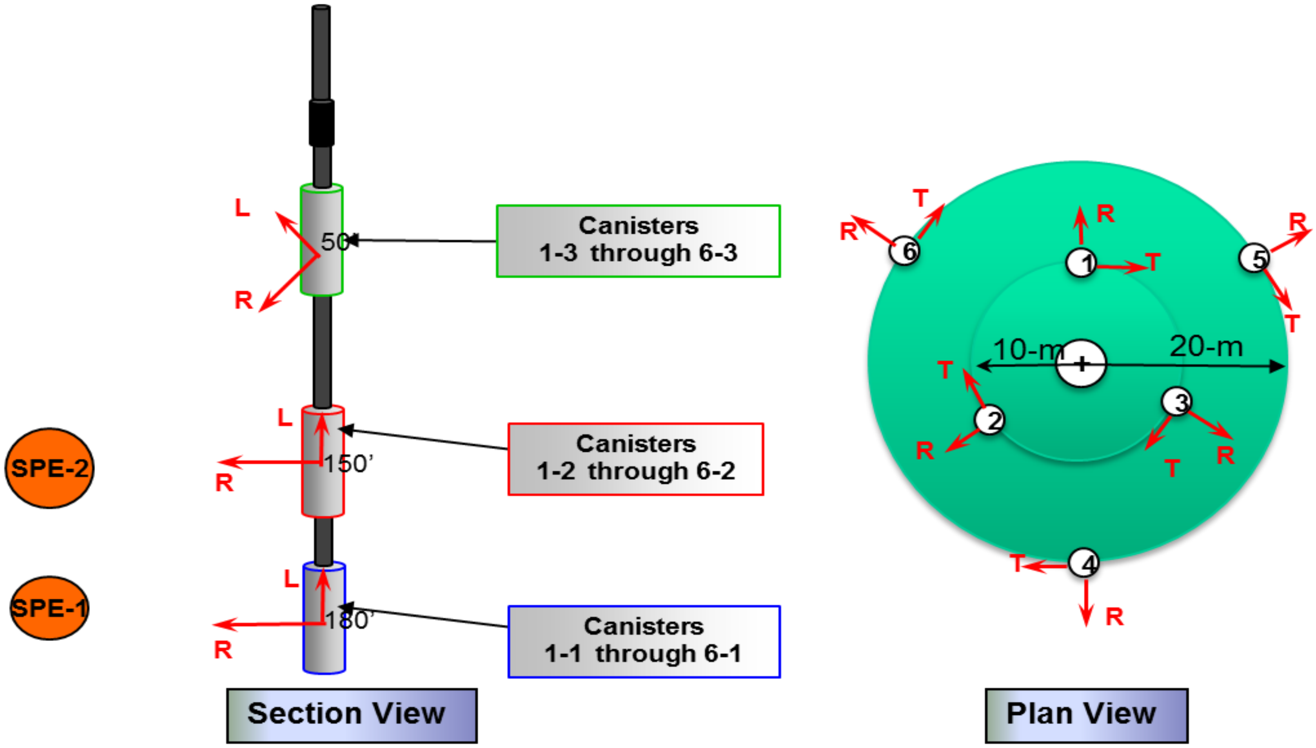

Figure 9: SPE-1/SPE-2 test layout

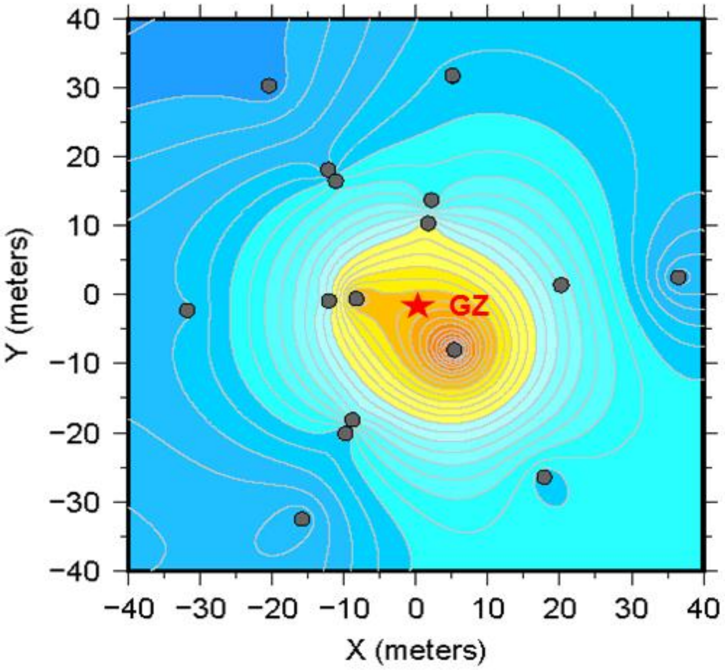

Figure 10: Contour plot of corrected peak radial velocity data for SPE-2 projected onto the shot plane.

Regardless, these data clearly define a peak velocity environment that is circular in nature with no apparent perturbation related to joints. This observation concurs with the ground shock in the JOLT event suggesting that we should not expect the SPE joint sets to alter the shape of the shock front emanating from these cylindrical explosive sources.

SUMMARY

The goal of the Shock Physics Experiments is to increase our understanding of the shock phenomenology from an explosive event to aid in modeling these events. A more accurate understanding of the effects of near source geology on that phenomenology is critical. We demonstrated the use of the multi-physics Abaqus® fully coupled Euler-Lagrange code to model the DTRA JOLT experiment. Abaqus/CEL was able to compute the high-deformation explosive loading, the complex rock response with damage, and the large general contact domain. Comparison of results to test data reveals that the simulation performed credibly.

These results provide insight into propagati0n of explosive-caused shock in jointed media. This exercise provides evidence that the shock front is not perturbed by the joints. While it is possible that later time, lower amplitude portions of the waveform can exhibit behavior caused by joints, we conclude that the main shock events from the SPE events is not effected by the local jointing.

REFERENCES

1. Gran, J.K., and Erlich, D. C., Jointed Limestone Tunnel (JOLT) Tests, DTRA-TR-07-16, SRI International, Menlo Park, CA, March 2007.
2. Lee, E.L., Hornig, H.C., and Kury, J.W., “Adiabatic Expansion of High Explosive Detonation Products,” UCRL-50422, Lawrence Radiation Laboratory, Livermore, CA, 1 May 1968.
3. Chitty, D. E., “Salem Limestone Properties to Support Calculation of the SRI Lab Scale Tests,”
4. Applied Research Associates, Inc., Memorandum to TTD ACTD Computation Group, South
5. Royalton, VT, 11 February 2004.
6. Steedman, D.W., and Swift, R.W., “Modeling Underground Structure Vulnerability in Jointed Rock,” Proceedings, 71st Shock and Vibration Symposium, Crystal City, VA, 2000.
7. Senseny, P.E., and Simons, D.A., “Comparison of Calculational Approaches for Structural Deformation in Jointed Rock,” International Journal for Numerical and Analytical Methods in Geomechanics, Vol. 18, 1994.